# Investigation of Mechanical and Metallurgical Properties on Mild Steel (St 52) and Aluminum (AA3003-H14) Friction Stir Welded Joints

Supraja Reddy. B [1*], Sumalatha. M [2], Avinash. P [3] and Yeshurun . P [4]

[1] Assistant Professor, Mechanical Engineering Department, V.R.Siddhartha Engineering College, Vijayawada, India.

[2] Assistant Professor, Mechanical Engineering Department, V.R.Siddhartha Engineering College, Vijayawada, India.

[3] UG Scholar, Mechanical Engineering Department, V.R.Siddhartha Engineering College, Vijayawada, India.

[4] UG Scholar, Mechanical Engineering Department, V.R.Siddhartha Engineering College, Vijayawada, India.

**Keywords:** Friction stir Welding, Dissimilar metals, Process parameters, Tensile strength, Hardness

**Abstract.** Non-coolant assisted and coolant assisted friction stir welding are used to weld dissimilar welded joints of Mild Steel (ST52) and AA3003-H14 aluminum alloy in this study. When using the classic Friction Stir Welding procedure, compare non-coolant assisted samples to coolant assisted samples. The impact of tool and rotating speeds on welded joints was investigated in this study. Using the tungsten carbide conical pin tool, this job is done at three rotating speeds of 900Rpm, 1120 Rpm and 1400 Rpm with a constant feed rate of 16 mm/min. The study finds that the tool material, Shoulder diameter, tool shape and material flow enhance the joint strength of dissimilar aluminum to mild steel welded samples. The results shown that joint welded at rotational speed of 1120 Rpm, pin offset of 0.3mm towards steel condition was defect less with a maximum tensile ultimate strength of 116.6 MPa. The cooling assisted samples were lower tensile strength compared to non-coolant assisted friction stir welded joints because of their surface defects and area c/s defects such as voids, tunnel defects, coarse grain structure and non-uniform distribution of the steel fragments and micro cracks formed in the interface of the dissimilar joints. Microstructures of stirred zone are seen in Steel/Al welded joints.

## INTRODUCTION

Due to their vastly different thermo physical qualities, such as heat conductivity and melting temperature, dissimilar connecting of aluminum alloys and steel alloys for light weight constructions remains difficult. Reduce the weight to improve energy efficiency and lower energy costs [1]. One of the weight-saving approaches used is to replace steel parts with lighter materials such as aluminium and its alloys. [2]. As observed in the study, connecting aluminum alloys with different types of steel alloys has been performed using both traditional and unusual FSW procedures. For example, Gas metal arc welding and shield metal arc welding are the most commonly utilised Materials welding processes in the shipbuilding sector. However, the demand for high quality welds, the need to remove produced slag, after welding, cold cracking, and work piece distortion induced by standard welding techniques have fueled the quest for alternative welding methods.

Friction stir welding is a solid - state metal joining technology with various advantages over competing processes, including lower energy input and less part distortion. As demonstrated in figure 1, this technique has shown significant promise in the joining of dissimilar metals, a methodology that is widely find after in the aerospace and automobile industries for its promised weigth-saving possibilities. The FSW allows for more exact heat input control during welding, preventing extra growth of the inter metallic layer and achieving the necessary mechanical qualities [3].

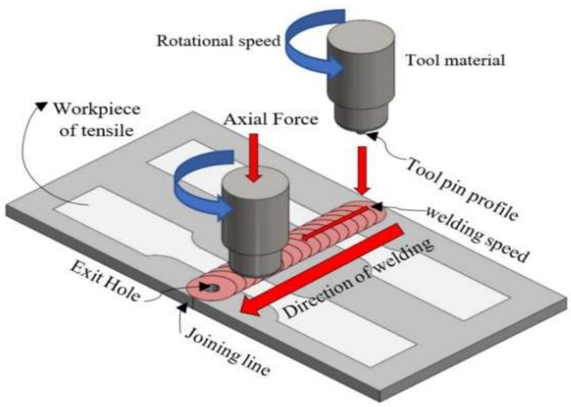


Fig. 1, Friction Stir Welding Process

Derek Shaffer et al. [4] investigated the use of EAFSW techniques to link Aluminum 6061-T651 to mild steel. XSYTIN-1, a unique tool made of proprietary ceramic, is also being tested in this application. Although EAFSW enhanced material flow between the constituent materials, it was unable to improve the weld joint strength. Furthermore, while comparing the XSYTIN-1 tool to a standard steel tool, no significant changes were discovered. The EADFSW method did not create stronger welds between dissimilar materials than the usual method. Although certain regions witnessed an increase in porosity, it did reduce voids and inconsistencies throughout the weld joint. This occurred owing to the increased material flow caused by the electricity, as well as the possibility of gas bubbles escaping due to higher warmth. To improve welded joint strength and mixing the steel's ductility must be changed with electricity or by raising the temperature to nearly match that of aluminum.

AmlanKar and colleagues .[5] With the use of comprehensive microstructure evaluation in FSLW of AA6061 and mild steel, the effect of interfacial microstructure at the welded joint interface mechanical characteristics was explored (MS). They discovered that at lower tool rotation speeds, where plastic deformation is less severe, the weld interface revealed a simple interface without an extended interlayer, and the fracture locations in the MMZ and intercalated structure revealed the high and low lap shear strength, respectively.

Mohamed M. Z. Ahmed et al. [6] investigated the metallurgical and mechanical properties of Friction Stir Welded joints made with Mild steel with a thickness of 5mm. They discovered that the simple shear texture dominates the crystallographic texture, which is the characteristic texture of friction-stir-welded materials, and that the hardness of the joints increased in the NG zone, which is primarily due to the fine-grained structure created after FSW. In the present study discussed on effect of cooling assisted and non-cooling assisted systems on AA3003-H14 and Mild Steel (ST 52) dissimilar friction stir welded joints.

## MATERIALS & METHODS

A vertical milling machine was used to butt weld 3mm thick AA3003-H14 and Mild Steel sheets along their lengths. The table1 displays the chemical composition of dissimilar metals. A tungsten carbide tool was used to weld with a conical taper shape. This study used a conical tool with pin measures of 6mm at the top and 4mm at the bottom. The tool's shoulder breadth and pin length were 20mm and 2.6mm, respectively. The plates were positioned with mild steel on the moving side and AA3003-H14 aluminum alloy on the retreating side, with a probe tilting angle of $2^0$. The test setup is shown in Figures 2a & 2b, and the machine process parameters are listed in Table 2.

Table 1, Base Metal Chemical Compositions

| Chemical Composition of AA3003-H14 aluminium alloy | | | | | | | | | |
|---|---|---|---|---|---|---|---|---|---|
| Elements | Zn | Fe | Cu | Pb | Mn | Ti | Si | Co | Al |
| [%] | 0.046 | 0.402 | 0.104 | 0.002 | 1.041 | 0.122 | 0.192 | 0.015 | 98.076 |
| Chemical Composition of Mild Steel (ST 52) | | | | | | | | | |
| Elements | Al | C | Mn | P | Si | S | Fe | | |
| [%] | 0.02 | 0.22 | 1.6 | 0.04 | 0.55 | 0.04 | 97.53 | | |

Fig. 2, a) FSW Setup without coolant b) FSW Setup with coolant (water)

### Metallographic Examination

The welding experiments had a conventional interaction set up metallographically. Using an optical microscope, the material flow, joint interface, and grain structure were observed.

### Mechanical Testing

As shown in Fig. 3, the joint strength of the dissimilar welded joints was investigated using ASTM E8 criteria. Additionally, the hardness is used to establish a link between optimum metal mixing and joint strength.

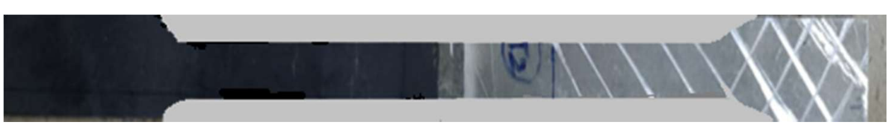

Fig. 3, Tensile Test specimen

Table 2, Process Parameters

| Method | Rotational Speed [Rpm] | Traverse Speed [mm/min] | Tool Geometry | Tool Material | Tilting Angle |
|---|---|---|---|---|---|
| Normal FSW | 900 | 16 | Cone | WC | $2^0$ |
| | 1120 | 16 | Cone | WC | $2^0$ |
| | 1400 | 16 | Cone | WC | $2^0$ |
| Cooling assisted FSW | 900 | 16 | Cone | WC | $2^0$ |
| | 1120 | 16 | Cone | WC | $2^0$ |
| | 1400 | 16 | Cone | WC | $2^0$ |

**RESULTS AND DISCUSSIONS**

**Weld appearance and Material Flow**

Figure 4(a&b) depicts the top surface of the coolant-assisted and non-assisted friction stir welded connections between steel and aluminium under different process parameters and tool geometries. The welded surface has shown the potential for both material discontinuity and volumetric defects to be produced as a result of excessive flash formation development in the joint interface.

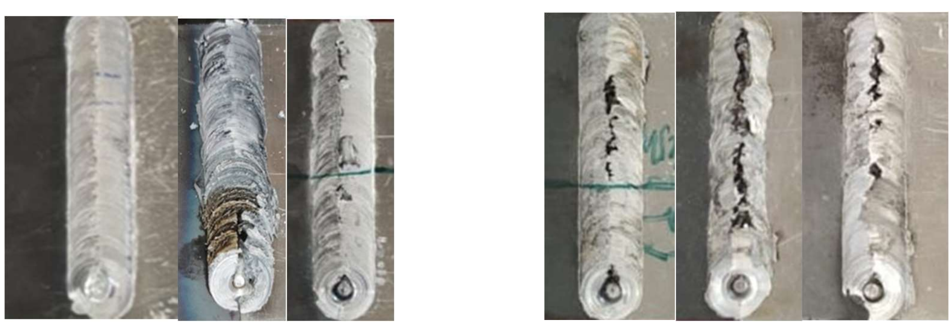

Fig. 4, (a) Non Coolant assisted FSW (b) Coolant assisted FSW

Figure 4 illustrates the impact of tool rotational speed, tool feed, tool material, and tool geometry on the look of the weld. Outwardly sufficient welded junctions were achieved when the rotating speed changed between 900 Rpm, 1120 Rpm, and 1400 Rpm and the tool form cone with a constant feed of 16mm/min. With a conical-shaped probe at 1120Rpm and a tool feed rate of 16mm/min, there were no surface flaws in the welded connection, however at 1400Rpm and a feed rate of 16mm/min, there were material discontinuities in the welded union. Figure 5 displays the many flaws in two circumstances.. Surface deformities created towards the aluminum side are addressed in Fig. 5(a), and voids shaped by improper material flow are addressed in Fig. 5(b).


Fig. 5, Blending of metals a) Normal Sample b) Coolant assistant sample

The whole material flow was initiated by the shoulder-induced flow under stirring conditions, and the vortex flow was subsequently produced by the flow pushed by the downward and upward tool pins [7]. Due to different mechanical, chemical, and thermal properties, dissimilar joining by FSW presents certain challenges [8, 9]. The typical friction stir joint exhibits 6(a) a smooth mixing of the base metals in the stirred zone and 6(b) some steel stretch in the aluminum side at the dissimilar joint's bottom [10].


Fig. 6, Surface flow of (a) Non-Coolant assisted FSW (b) Coolant assisted FSW

All joints exhibit this behaviour as the base metals contact shifts in favour of the aluminium side. Because of the high temperature and high material flow created at the top of the weld but insufficient temperature and flow at the nugget, the cooling aided samples exhibit more tunnel flaws at the nugget and joined at the top face of the weld. In comparison to normal conditions, the cooling media produces increased cooling rates; total material flow is restricted at the weld root, which results in less action of stirring and worse mechanical bonding at lower areas of the stirred zone. Due to the slower cooling rate than cooling media assisted dissimilar friction stir welded joints, the standard FSW welded joints did not exhibit any segregations. However, the increased heat concentration on the swirled zone resulted in proper material mixing and improved mechanical bonding.

In the image (figure 6 a & b), the surface flows of several joints are depicted. It was found that samples with coolant assistance generate rough surface flows at faster cooling rates. As can be observed, the viscosity of the material influences this surface behaviour. Materials directly in touch with the shoulder in all samples under more thermo-mechanical cycling than other regions, and viscosity of the materials varied surface flow rings. A focusing of materials on the joint line is indicated by the smaller spacing between flow rings created in Friction Stir Welding and the shorter cooling cycle. It appears that the Friction Stir welding tool shown in figure 7 applies more stress to the lower viscosity metals at the trailing edge, increasing the mixing of different materials at the joint's top.

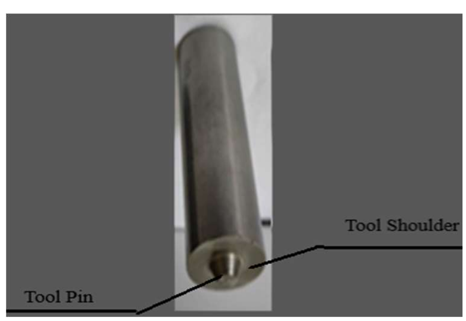


Fig. 7, Conical tungsten carbide tool

## Microstructure

The microstructures of the stirred zones in several samples—both those with and without coolant assistance—are depicted in the figure 8. The differences in grain size at both ends can be seen by studying the Stirred Zone. It appears that as the rate of cooling rises, so do the grain sizes. When coolant assistance is used, the grain size distribution is more uneven. Due to the tool offset is towards the steel, generating severe deformation in the surrounds, the grain refinement is higher on the steel side [11, 12]. The grain size of the steel and aluminum sides is continuously refined in comparison to lower rotational speeds of 900rpm and 1400rpm in the case of non-coolant assisted samples, where heat input generation is medium at 1120rpm and high at 1400rpm. Reducing the cooling rate then causes the formation of an interface of joint with coarse grains, as shown in Figure 8 (a,b,c).

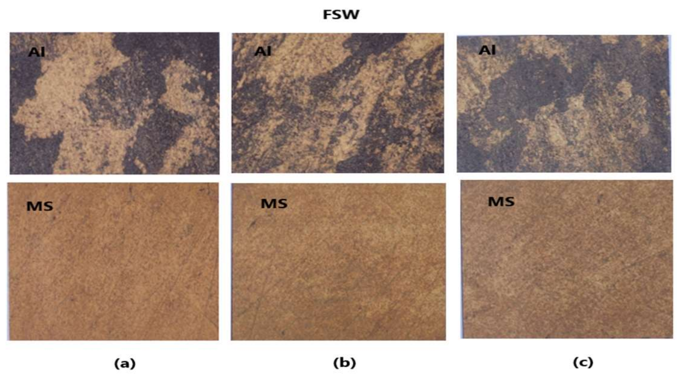


Figure. 8, Non-coolant assisted samples (a) Microstructure at 900 Rpm, (b) Micro structure at 1120 Rpm, and (c) Micro structure at 1400 Rpm

Because the shoulder has a larger diameter, the temperature there is typically greater than the temperature near the tool probe in the stirred zone. Because there is no intermetallic layer forming due to insufficient temperatures as illustrated in figure 9(a,b) the higher cooling rates along the agitated zone in the coolant aided samples leads to inappropriate metal mixing and poor grain development in the stirred zone. As a result, the grain size is smaller in samples without coolant assistance than in those with coolant assistance.

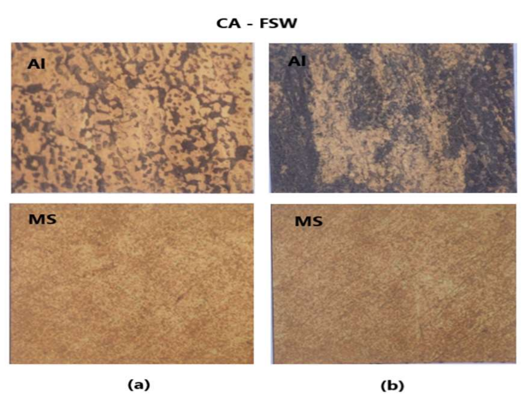


Fig. 9, Coolant assisted samples (a) Microstructure at 900 Rpm, (b) Micro structure at 1120 Rpm

**Mechanical strength**

Table3 displays the mechanical characteristics of steel to aluminum joints. Numerous studies have found that because steel and aluminum have different thermal expansion coefficients, there is a requirement for continuous bonding between grain structures that are less brittle, which is given by thin intermetallic layers. The effectiveness of a dissimilar welded joint depends on its tensile qualities, which are related to optimum material mixing, intermetallic layer thickness, and, additionally, constantly placing the harder material on the forward-moving side [13–15]. When utilising a conical tool without coolant, the execution of the tool probe rotational speed is medium compared to the tool feed rate, as this increases heat production and enhances the degree of mixing.

Table 3, Mechanical Properties

| Method | Tool Rotational Speed [Rpm] | Tool feed rate [mm/min] | Tensile strength [MPa] | Hardness [HBN] |
|---|---|---|---|---|
| Non - coolant assisted FSW | 900 | 16 | 73.3 | 80 |
| | 1120 | 16 | 116.6 | 84.86 |
| | 1400 | 16 | 33.3 | 150 |
| coolant assisted FSW | 900 | 16 | 56.6 | 75 |
| | 1120 | 16 | 66.6 | 79 |
| | 1400 | 16 | 27 | 120 |

As these produced defective junctions occur at 1400rpm and 16mm/min with the coolant, the probe rotational speed is higher. The weakest material flow and temperature in this work result in the coolant aided samples exhibiting poor mechanical strength bonding at the stirred zone, which also causes greater inhomogeneous shrinkage and distorts the joint interface to result in segregation as shown in the figure10. As a result, in the sample with coolant assistance, Due of improper mechanical bonding and more distortion, weld root cracks can be seen at the stirring zone. Due to low joint strength caused by bulk production of steel in the agitated zone, these samples displayed a significant degree of brittleness. The agitated zone's middle was where the fracture happened.

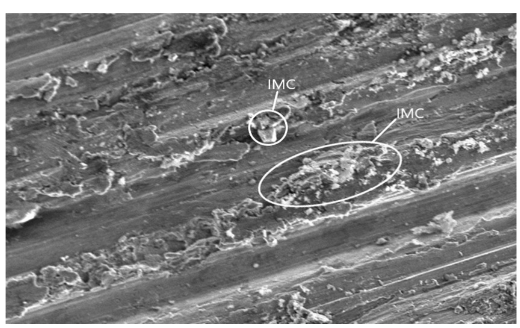


Fig. 10, Fracture surface of coolant assisted sample

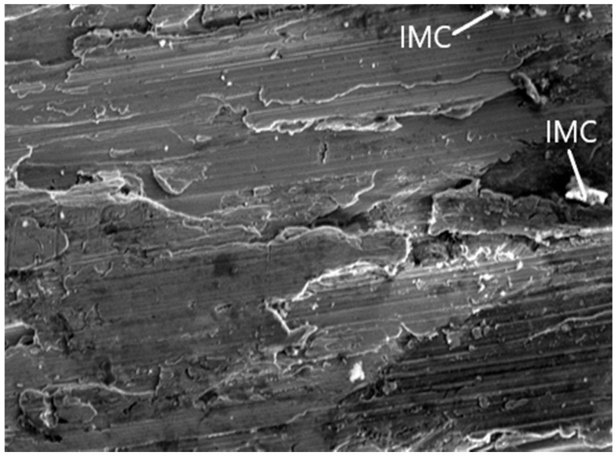


Fig. 11, Fracture surface of Non - coolant assisted sample

As a result of efficient material flow at the interface, a reduction in brittle phases, and proper mechanical bonding, as shown in the figure 11, the results demonstrate that non-coolant assisted samples had the maximum tensile strength when compared to coolant helped samples.. The production of intermetallic compounds at the contact of metals that are not comparable determines the hardness primarily. Steel is diffused with aluminum particles as they move from the advancing side, creating hard, brittle structures in the agitated zone. The coolant assisted welded samples show a diverse structure in the stirred zone's creation and distribution, including peaks and valleys. The Al/Steel interface zone, which was agitated in a zigzag pattern with steel particles embedded in the fracture surface, was where the tensile fraction was discovered. The weld joint failed in a brittle way, as evidenced by the large amount of material that was deposited at the break zone. The Thermo Mechanical Affected Zone showed the greatest change in hardness values between those measured in the stirred zone and soften region.

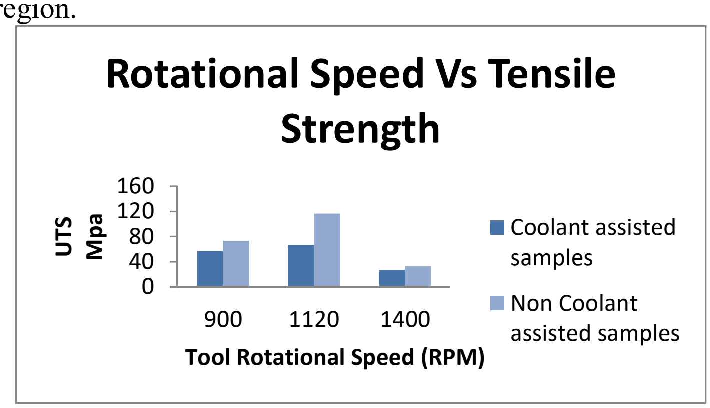


Fig. 12, Tensile Strength at various conditions

Figure12 had shown a tensile ultimate strength at different conditions. The strengthen joint is got at 1120rpm and 16mm/min with tungsten carbide conical probe in non-coolant assisted welded joints. Tensile strength is obtained at this condition is 116.6MPa. The imperfection welded joint is found at 1400Rpm and 16mm/min with tungsten carbide conical tool probe in coolant assisted welded joints. Figure 13 display the hardness of welded joints at various conditions. The extreme hardness is obtained at the non-coolant assisted joint in the interface zone. In this state, thick Inter Metallic layers are framed and diminished the joint strength. The less hardness is obtained at coolant assisted joint and at 1120 Rpm the hardness value is 84.86 HBN obtained a good joint.

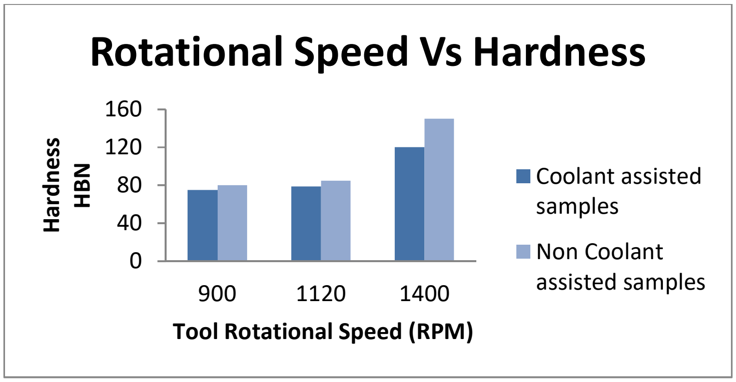


Fig. 13, Hardness of welded joints at different conditions

## CONCLUSIONS

Friction stir dissimilar welding of AA3003-H14 and Mild Steel (ST52) joints has been completed in this study. Following consideration of the relationship between the mechanical and metallurgical qualities of welded joints and the effect of coolant-assisted samples compared to non-coolant-assisted samples.

- The non-coolant assisted dissimilar joint's strong strength is a result of the metals' appropriate mixing during metallurgical bonding, which uses less hardness than mechanical bonding and proper material flow utilising a conical tool. Due to improper material flow, which results in low strength mechanical bonding in the agitated zone and excessive distortion, coolant-assisted samples have poor strength.
- Because there are many scattered steel pieces on the tensile fracture surface, the mode of failures occurs more frequently at coolant assisted welded joints than non-coolant assisted welded joints.
- The non-coolant assisted sample had a better tensile ultimate strength of 116.6MPa at a tool rotational speed of 1120Rpm than the coolant assisted welded joint, which had a tensile ultimate strength of 66.6MPa. This was due to insufficient heat; since the coolant was continuously flowing over the weld surface, the required temperature may not have been reached, causing voids to form.
- Due to incorrect mixing brought on by insufficient temperature, created voids, and blowholes, the non-coolant aided sample with 900 Rpm rotating speed exhibits reduced strength. With regard to the coolant assisted sample effect on the 900 Rpm specimen, the heat input for welding is further lowered as a result of the coolant flowing continuously over the weld surface during welding. This results in faulty welding and poorer strength.
- Due of the high rotational speed, highly plasticized aluminum, and imperfect mixing, the non-coolant specimen at 1400 Rpm likewise displayed inferior strength. The strength of a 1400 Rpm specimen was also lessened by the coolant's influence because cracks developed as a result of the quick cooling of the high temperatures in the weld zone that were made possible by the high rotating speed.
- This study demonstrates that because there is no connection between the steel faying surface and the conical tool probe at the bottom area of the weld, conical probes are not suited for welding aluminum to steel for butt joints.

**REFERENCES**

[1] E. Schubert, M. Klassen, I. Zerner, C. Wlaz, and G. Sepold (2001) Laser beam joining produces light-weight structures for future automotive and aerospace applications. 115:2–8 J Mater Process Technol.

[2] The suitability of aluminium as an alternative material for automobile bodywork, Carle D, Blount G (1999). 267–272 in Mater Des.

[3] H-S Bang, SM Hong, A Das, H-S Bang (2019) TIG assisted hybrid friction stir welding was used to investigate the weldability and mechanical properties of different materials (Al5052-DP590). 1–12 in Metals and Materials International.

[4] IhabRagai, Derek Shaffer, Tyler J. Grimm, and John Roth Advanced Materials Research, SSN: 1662-8985, Vol. 1152, pp 31-41, "Utilization of XSYTIN-1 Tool in Electrically-Assisted Friction Stir Welding of Dissimilar Metals Al 6061-T651 to Mild Steel."

[5] Materials Characterization 168 (2020) 110572 Amlan Kara, BuchibabuVicharapua, Yoshiaki Morisada, and Hidetoshi Fujii "Elucidation of interfacial microstructure and characteristics in friction stir lap welding of aluminium alloy and mild steel".

[6] Mohamed M. Z. Ahmed, Mohamed M. El-SayedSeleman, Kamel Touileb, Ibrahim Albaijan, and Mohamed I. A. Habba are among those who have contributed to this work. Materials 2022, 15, 2905, "Microstructure, Crystallographic Texture, and Mechanical Properties of Friction Stir Welded Mild Steel for Shipbuilding Applications." https://doi.org/10.3390/ma15082905.

[7] Chitturi, V.; Pedapati, S.R.; Awang, M. Effect of Tilt Angle and Pin Depth on Dissimilar Friction Stir Lap Welded Joints of Aluminum and Steel Alloys. Materails 2019, 12, 3901.

[8] Heirani, F.; Abbasi, A.; Ardestani, M. Effects of processing parameters on microstructure and mechanical behaviors of underwater friction stir welding of Al5083 alloy. J. Manuf. Process. 2017, 25, 77–84.

[9] Wang, Q.; Zhao, Z.; Zhao, Y.; Yan, K.; Zhang, H. The adjustment strategy of welding parameters for spray formed 7055 aluminum alloy underwater friction stir welding joint. Mater. Des. 2015, 88, 1366–1376.

[10] Abd Elnabi, M.M.; Osman, T.A.; El Mokadem, A.; Elshalakany, A.B. Evaluation of the formation of intermetallic compounds at the intermixing lines and in the nugget of dissimilar steel/aluminum friction stir welds. J. Mater. Res. Technol. 2020, 9, 10209–10222.

[11] Tan, Y.B.; Wang, X.M.; Ma, M.; Zhang, J.X.; Liu, W.C.; Fu, R.D.; Xiang, S. A study on microstructure and mechanical properties of AA 3003 aluminum alloy joints by underwater friction stir welding. Mater. Charact. 2017, 127, 41–52.

[12] Papahn, H.; Bahemmat, P.; Haghpanahi, M.; Sommitsch, C. Study on governing parameters of thermal history during underwater friction stir welding. Int. J. Adv. Manuf. Technol. 2015, 78, 1101–1111.

[13] Zhao, Y.; Jiang, S.; Yang, S.; Lu, Z.; Yan, K. Influence of cooling conditions on joint properties and microstructures of aluminum and magnesium dissimilar alloys by friction stir welding. Int. J. Adv. Manuf. Technol. 2016, 83, 673–679.

[14] Zhang, Z.; Yu, Y.; Zhao, H.; Tong, H. Effect of Loading Methods on the Fatigue Properties of Dissimilar Al/Steel Keyhole-Free FSSW Joints. Materails 2020, 13, 4247.

[15] Zhang, J.; Shen, Y.; Yao, X.; Xu, H.; Li, B. Investigation on dissimilar underwater friction stir lap welding of 6061-T6 aluminum alloy to pure copper. Mater. Des. 2014, 64, 74–80.